Am J Cancer Res 2020;10(1):299-313
www.ajcr.us /ISSN:2156-6976/ajcr0106095

Original Article

USP7 stabilizes EZH2 and enhances cancer malignant progression

Nana Zheng[1,3*], Man Chu[1*], Min Lin[1], Youhua He[2], Zhiwei Wang[1,3]

Departments of [1]Obstetrics and Gynecology, [2]Urology, The Second Affiliated Hospital of Wenzhou Medical University, Wenzhou 325027, Zhejiang Province, China; [3]Department of Pathology, Beth Israel Deaconess Medical Center, Harvard Medical School, Boston, MA, USA. [*]Equal contributors.

Received November 24, 2019; Accepted December 22, 2019; Epub January 1, 2020; Published January 15, 2020

Abstract: EZH2, a histone methylase, plays a critical role in the tumor progression via regulation of progenitor genes. However, the detailed molecular mechanism of EZH2 in cancer malignant progression remains unknown. Therefore, we aimed to investigate how EZH2 is regulated in human cancer. We used numerous approaches, including Co-immunoprecipitation (Co-IP), Transfection, RT-PCR, Western blotting, Transwell assays, and animal studies, to determine the deubiquitination mechanism of EZH2 in cancer cells. We demonstrated that USP7 regulated EZH2 in human cancer cells and *in vivo* in mouse models. Overexpression of USP7 promoted the expression of EZH2 protein, but overexpression of a USP7 mutant did not change the EZH2 level. Consistently, knockdown of USP7 resulted in a striking decrease in EZH2 protein levels in human cancer cells. Functionally, USP7 overexpression promoted cell growth and invasion via deubiquitination of EZH2. Consistently, downregulation of USP7 inhibited cell migration and invasion in cancer. More importantly, knockdown of USP7 inhibited tumor growth, while USP7 overexpression exhibited opposed effect in mice. Our results indicate that USP7 regulates EZH2 via its deubiquitination and stabilization. The USP7/EZH2 axis could present a new promising therapeutic target for cancer patients.

Keywords: USP7, EZH2, cancer, metastasis, invasion

Introduction

In the United States, prostate cancer is the most commonly diagnosed cancer in males, and it is the secondary highest cause of mortality worldwide, despite of the progressive decline in incidence and death rates [1]. Like many other cancers, prostate cancer progresses from a nonaggressive and slow-growing stage to an aggressive and fast-growing stage that requires treatment [2]. The prostate-specific antigen (PSA) level has been widely used for the early detection of prostate cancer, sometimes in combination with a digital rectal examination or other ancillary tests [3]. However, these detections cannot discriminate between nonaggressive tumors and aggressive tumors, and the molecular mechanism of prostate tumorigenesis remains unknown. Therefore, it is important to elucidate the mechanism of prostate carcinogenesis.

The ubiquitin-proteasome system (UPS) controls the degradation of targeted proteins and plays critical roles in cell proliferation, apoptosis, migration, invasion and the cell cycle [4, 5]. It has been reported that the UPS governs approximately 80% to 90% of the protein degradations that occurs in cells [6]. The degradation of proteins requires two processes: conjugation of ubiquitin to the targeted substrates and degradation of the ubiquitinated proteins [7]. Three types of enzymes, E1, E2, and E3, catalyze the degradation process. Specifically, the E1 enzyme activates ubiquitin molecules and transfers them to the E2 enzyme, and subsequently the activated ubiquitin molecules are recruited to the E3 ligases. The E3 complex binds to substrate proteins, and the ubiquitinated substrates are further degraded by 26S proteasomes [7]. Ubiquitination mediates targeted protein degradation, while deubiquitylases (DUBs, also called deubiquitinases) can remove ubiquitin from labeled proteins or from polyubiquitin chains and maintain targeted protein stability [6]. Therefore, DUBs can reverse the function of E3 ligases and contribute to the turnover of substrate proteins, thus exhibiting a

significant effect on cellular processes. In turn, irregular DUB expression has a close relationship with migration, invasion and carcinogenesis.

The human genome encodes at least 98 DUBs and they are categorized into 6 subfamilies: USPs (ubiquitin-specific proteases), UCHs (ubiquitin carboxyl-terminal hydrolases), OTUs (ovarian-tumor proteases), MJDs (Machado-Joseph disease protein domain proteases), JAMMs (JAMM/MPN domain-associated metallopeptidases) and MCPIPs (monocyte chemotactic protein-induced proteases) [8-10]. Among all the DUB subfamilies, the USP family is the largest with approximately 60 members. Among the USP members, USP7 is the most well characterized [11]. USP7, ubiquitin specific protease 7 (also known as HAUSP), can reverse ubiquitination and spare substrate proteins from degradation [12]. For example, USP7 has been shown to deubiquitinate MDM2, which functions as an ubiquitin ligase (E3) that directly mediates the ubiquitination and subsequent degradation of p53. However, depletion of USP7 promotes the degradation of MDM2, and subsequently stabilizes p53, thus inhibiting the cell cycle and promoting apoptosis [13-15].

Enhancer of zeste homolog 2 (EZH2) is a catalytic subunit of PRC2 (Polycomb repressive complex 2), which silences gene expression via methylation of lysine 27 of histone H3 [16, 17]. It has been reported that EZH2 downregulates tumor suppressors, such as ADRB2 and DAB2IP, and subsequently leads to malignant progression of CRPC (castration-resistant prostate cancer) [18, 19]. Additionally, EZH2 also affects oncogenes, including Ras, NF-κB and AR, in metastatic prostate cancer [16, 17, 20]. Posttranslational modifications of EZH2 such as ubiquitination, SUMOylation, phosphorylation and glycosylation, also influence its stability and oncogenic activity. The ubiquitination of EZH2 has an effect on the activity of PRC2 in cancers [21]. Studies have shown that β-TrCP, Praja1 and Smurf2 function as ubiquitin E3 ligases for EZH2 in lymphoma, breast cancer and neuron differentiation, respectively [22-25]. However, the molecular mechanism of EZH2 in prostate cancer is still elusive.

In this study, we investigated the relationship between USP7 and EZH2. We found that USP7 stabilized EZH2 via deubiquitination in human prostate cancer cells. Overexpression of USP7 enhanced the stability of EZH2, while deletion of USP7 decreased the EZH2 protein level and thus suppressed prostate tumorigenesis. Our work suggested that USP7 is a novel regulator of EZH2, and that targeting the USP7/EZH2 pathway could be a promising therapeutic approach for patients with prostate cancer.

Methods and materials

Cell culture and reagents

Human DU145, PC3, 293T, HeLa and T98G cells were cultured in DMEM with 10% fetal bovine serum and 1% penicillin and streptomycin in a 5% CO_2 atmosphere at 37°C. LNCaP cells were cultured in RPMI1640 supplemented with 10% fetal bovine serum and 1% penicillin and streptoMycin at 37°C in 5% CO_2. The primary antibody for EZH2 (ab228697) was purchased from Abcam Company (Cambridge, MA, USA). USP7 antibody was purchased from Santa Cruz Company (Santa Cruz, CA, USA). Anti-Flag and anti-Myc antibodies were obtained from Sigma-Aldrich (St. Louis, MO, USA). All secondary antibodies were obtained from Thermo Scientific. Lipofectamine 2000 was purchased from Invitrogen. Monoclonal anti-tubulin was obtained from Sigma-Aldrich. CTG (Cell Titer-Glo) Luminescent was purchased from Promega (Madison, WI, USA). Matrigel and Transwell inserts were purchased from BD Biosciences. ShRNA vectors to deplete endogenous EZH2 were purchased from GenePharma (Shanghai, China).

Transfection

Cells were cultured in 6-well plates overnight and transfected with Myc-EZH2 cDNA, Flag-EZH2 cDNA or shRNA, Flag-USP7 cDNA or shRNA, and a combination or empty vector using Lipofectamine 2000 following the manufacturer's protocol. USP7-C223S was transfected into the cells using Lipofectamine 2000. After 4-6 h, the medium was replaced with fresh DMEM. The cells were harvested at 48 h for further analysis, which are described in the results sections.

Immunoprecipitation

293T, T98G, PC3 and DU145 cells were transfected with Flag-USP7, Flag-EZH2, or pcDNA3.0

as an empty vector. Then, the harvested cells were lysed for 30 min in protein lysis buffer (Sigma-Aldrich) on ice. After centrifugation, the protein concentration was detected by a BCA Protein Assay kit (Thermo Scientific, MA). The immunoprecipitation of FLAG-tagged proteins was performed by using a FLAG (M2) affinity gel incubated overnight. After precipitation, the beads were washed three times with protein lysis buffer and then combined with 30 μl of 2× loading buffer (1:1). The samples were boiled for 5 min at 95°C and loaded onto the SDS-PAGE gels [21].

In vivo deubiquitination assay

HeLa or 293T cells were transfected with or without HA-tagged ubiquitin, Myc-EZH2 and desired constructs. After 36 h of transfection, cells were treated with 20 μM MG132 for 10 h. Cells were lysed in lysis buffer containing 150 mM NaCl, 20 mM Tris-HCl (pH 7.4), 1% Nonidet P-40, 0.5 mM EDTA, PMSF (50 μg/ml), N-ethylmaleimide (10 mM) and protease inhibitors. After centrifugation, the anti-Myc antibody and protein A/G plus agarose beads were added to the supematants, and the mixture was incubated at 4°C for 16 h. The beads were washed with lysis buffer 6 times and combined with 2× loading buffer. Boiled beads were used for standard immunobloting.

Cell viability assay

Exponentially growing cells were seeded in 96-well plates (3×10^3 cells/well) overnight. Then the cells were transfected with Flag-USP7 or USP7-shRNA, and the medium was replaced with fresh medium after 6 h. After 48 h, 20 μl CTG solution was added to each well and cell viability was measured by a microplate reader. Each value was normalized to that of cells transfected with empty vector.

Cell apoptosis analysis

PC3 cells were cultured in 6-well plates overnight. The cells were transfected with EZH2-shRNA, Flag-USP7 or both. The empty vector was transfected as a control group. After 48 h, cells were collected and washed with PBS, and the cells were resuspended in 500 μl of binding buffer with 5 μl of propidium iodide (PI) and 5 μl of FITC-conjugated anti-Annexin V antibody. Subsequently, apoptosis was detected by a FACSCalibur flow cytometer (BD, USA).

Cell invasion assay

To determine the invasive ability of prostate cancer cells, Transwell assays were performed using PC3 and DU145 cells. Cells transfected with USP7 cDNA, USP7-shRNA, EZH2 shRNA or a combination of USP7 cDNA and EZH2 shRNA were cultured in 200 μl serum-free medium in the Matrigel-coated upper chamber. Complete medium with 10% FBS was added to the lower chamber. Cells were incubated for 20 h at 37°C with 5% CO_2, and the cells that had adhered to the bottom chamber were stained with Giemsa and were taken pictures.

Cell scratch assay

PC3 and DU145 cells were seeded in 6-well plates and transfected with desired plasmids. After the cells were almost 100% confluent, then the cells were scratched with a sterile 20 μl pipette tip. The cells were washed with PBS and fresh medium was added. The scratch was imaged with a microscope at 0 h and 20 h.

Quantitative real-time reverse transcription-PCR analysis

Total RNA was extracted with Trizol (Invitrogen, Carlsbad, CA) and reversed-transcribed into cDNA via a RevertAid First Strand cDNA Synthesis Kit. PCR was performed using Power SYBR Green PCR Master Mix and the results were calculated by the $2^{-\Delta\Delta Ct}$ method. The primers used in the PCR are as follows: EZH2, forward primer (5'-GTGGAGAGATTATTTCTCAA-GATG-3') and reverse primer (5'-CCGACATA-CTTCAGGGCATCAGCC-3'). GAPDH, forward primer (5'-ACCCAGAAGACTGTGGATGG-3') and reverse primer (5'-CAGTGAGCTTCCCGTTCAG-3').

Western blotting analysis

Cells were collected, washed with PBS and lysed by protein lysis buffer on ice. After centrifugation, the protein concentration was detected by a BCA Protein Assay kit (Thermo Scientific, Waltham, MA, USA). Equal amounts of protein were loaded into in sodium dodecyl sulfonate (SDS) polyacrylamide gel, separated by electrophoresis, and then transferred onto a polyvinylidene fluoride (PVDF) membrane. The membranes were then incubated with primary antibody at 4°C overnight. The membrane was washed three times with TBST and incubated with a second antibody for 1 h at room temper-

ature. Then, the expression of protein was detected by electro-chemiluminescence (ECL) assay.

Mouse xenograft assay

6×10^6 PC3 cells with USP7 overexpression or USP7 knockdown and control cells were suspended in 100 μl of DMEM mixed with Matrigel and injected into the flanks of male nude mice. Tumor size and weight were determined every 2 d, and the tumor volume was measured according to the formula: $L\times W^2\times0.52$, where the *L* represents the longest diameter and the *W* is the shortest diameter. At the end of the study, the mice were killed and the tumors were resected. Tumor volume and weight were measured as mentioned above.

Immunohistochemistry

Prostate cancer tumor samples or xenograft tumors were deparaffinized, dehydrated and incubated in heat-mediated antigen retrieval solution. Subsequently, the slides were cooled to RT and incubated with 3% H_2O_2 for 10 min to block endogenous peroxidase activity. After washing, the slides were incubated in normal bovine serum (Biosharp) to block nonspecific binding of IgG. Then, the slides were treated with primary antibody USP7 and EZH2 at 4°C overnight. Slides were washed and incubated with streptavidin-conjugated horseradish peroxide in PBS for 1 h at RT. After washing with PBS 3 times, the slides were treated with DAB for 5 min. Images were acquired by an Olympus camera and matched software. IHC straining was scored by two independent pathologists on the basis of the "most common" criteria.

Statistical analysis

All statistical analyses were conducted using GraphPad Prism 5.0 (Graph Pad Software, La Jolla, CA). Student's *t*-test and ANOVA were performed to evaluate statistical significance. The results are presented as the means ± SD. $P<0.05$ was considered statistically significant.

Results

The histone methylase EZH2 physically associates with the deubiquitinase USP7

To explore the association between EZH2 and USP7, Flag-USP7 and Myc-EZH2 were both transfected into PC3, DU145 and T98G cells. The external expression of Myc-EZH2 was higher than that in the control group due to the transfection of USP7 (**Figure 1A**). The expression of EZH2 was increased in a dose-dependent manner according to USP7 levels (**Figure 1B**). To explore the potential of USP7 to modulate the stability of EZH2, the cycloheximide (CHX) chase assay was performed to detect the half-life of EZH2. In this experiment, PC3 and HeLa cells were transfected with USP7 cDNA and incubated with CHX. The cells were collected at different time points. The Western blotting results indicated that overexpression of USP7 extended the half-life of EZH2 (**Figure 1C**). USP7/C223S is a catalytically inactive mutant of USP7. When the wild-type and mutant USP7 were transfected into DU145, HeLa and T98G cells, expression of EZH2 was higher in cells transfected with the wild-type USP7 transfection than in cells transfected with USP7/C223S or control group (**Figure 1D**). The protein level of EZH2 was decreased when cells were transfected with EZH2-shRNA, while the level of EZH2 was rescued when USP7 cDNA was transfected (**Figure 1E**).

To further determine the physical interaction between EZH2 and USP7, co-immunoprecipitation (Co-IP) experiments were performed. The Flag-USP7 or Flag-EZH2 was transfected into DU145 and 293T cells. After 48 h, the cells were harvested and lysed on ice. The Flag-M2 beads were added to the supernatant overnight. The samples were detected by Western blotting assay and IB with antibody against USP7 revealed that USP7 was co-immuoprecipitated with EZH2 (**Figure 1F**, **1G**). Similarly, IB with the EZH2 antibody result suggests that EZH2 co-immuoprecipitated with USP7 (**Figure 1F**, **1G**).

USP7 promotes the stabilization of EZH2

To determine the function of the interaction between USP7 and EZH2, we detected the effect of USP7 deletion on the EZH2 level. Two different sets of USP7 shRNA were transfected into multiple cells, and the IB result showed that the EZH2 protein level was reduced as a consequence of the USP7 deletion (**Figure 2A**, **2B**). In addition, the decrease in EZH2 levels caused by USP7 knockdown occurred only at the protein level and was not a result of reduced mRNA levels (Supplementary Figure 1). RT-PCR demonstrated that USP7 deletion did not lead

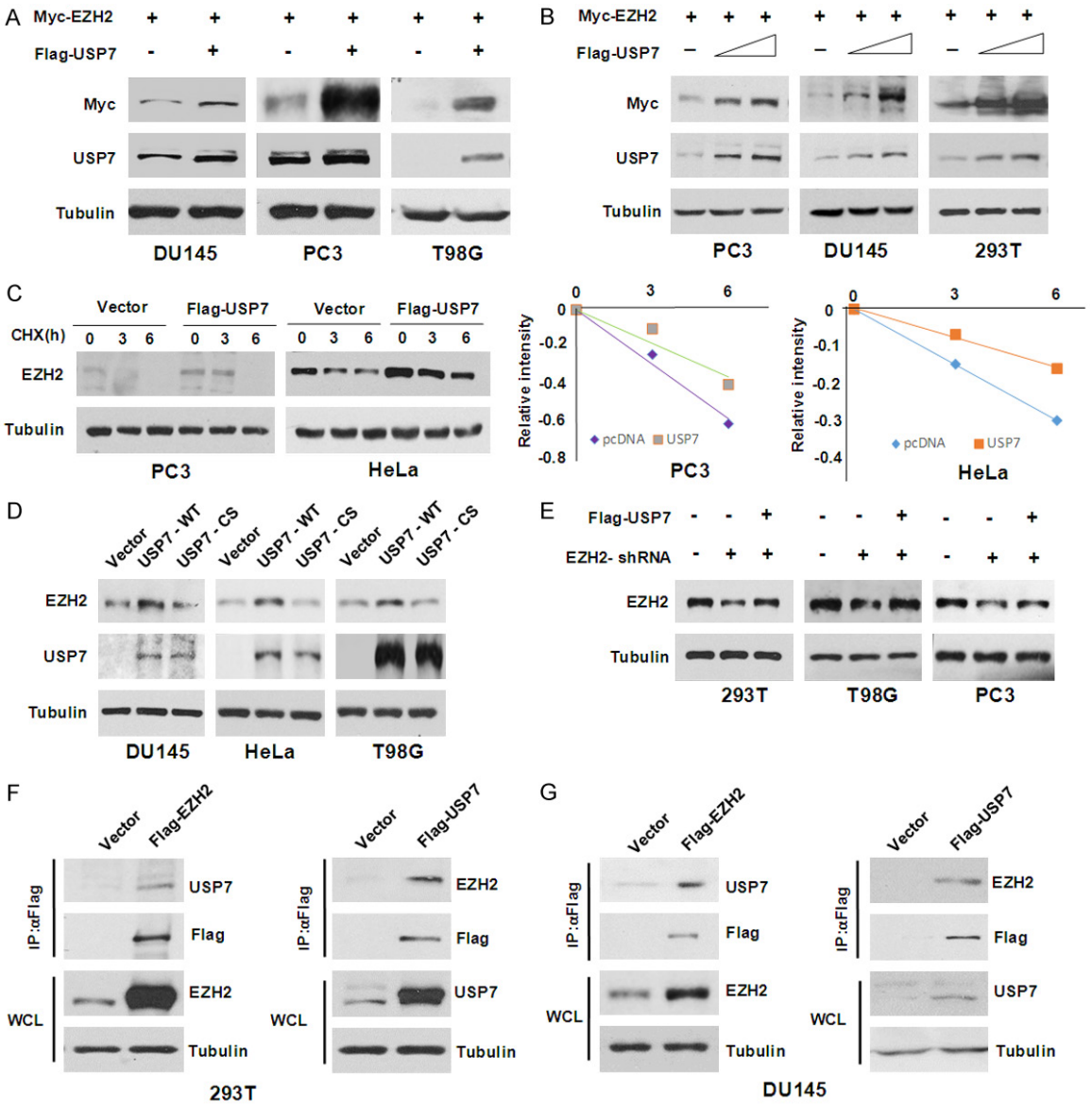

Figure 1. The deubiquitinase USP7 physically associates with the histone methylase EZH2. (A) PC3, DU145 and T98G cells were transfected with Myc-EZH2 and Flag-USP7. Cellular extracts were collected for Western blotting. (B) PC3, DU145 and 293T cells were transfected with Myc-EZH2 and different doses of Flag-USP7. Cellular extracts were collected for Western blotting. (C) Left panel, PC3 and HeLa cells transfected with empty vector and USP7 cDNA constructor were treated with cycloheximide (CHX; 50 mg/ml), harvested at specific time points, and then analyzed by Western blotting. Right panel, Quantitative results are illustrated for the left panel. (D) DU145, HeLa and T98G cells were transfected with USP7-WT, USP7-C223S and empty vector, harvested and analyzed by Western blotting. (E) 293T, T98G and PC3 cells were transfected with EZH2-shRNA or a combination of EZH2-shRNA and USP7 cDNA or an empty vector. Then, Western blotting analysis was performed. (F) Flag-EZH2 or Flag-USP7 was transfected into 293T cells, and cellular extracts were immunoprecipitated with anti-FLAG followed by IB. (G) Experiments analogous to those in part (F) were performed in DU145 cells transfected with Flag-EZH2 or Flag-USP7.

to the changes in EZH2 mRNA levels in multiple cells (Supplementary Figure 1). Furthermore, the USP7-dependent degradation of EZH2 was efficiently blocked by the proteasome inhibitor, MG132, suggesting that USP7 regulated EZH2 protein levels through the ubiquitin proteasome pathway (**Figure 2C**). These results indicated that USP7 governs the stability of EZH2 and the EZH2 is a substrate of USP7. To further define the effect of USP7 deletion on the EZH2 level, CHX assays were performed. The 293T and T98G cells were transfected with control shRNA and USP7-shRNA, and then incubated with CHX. The cells were harvested at different

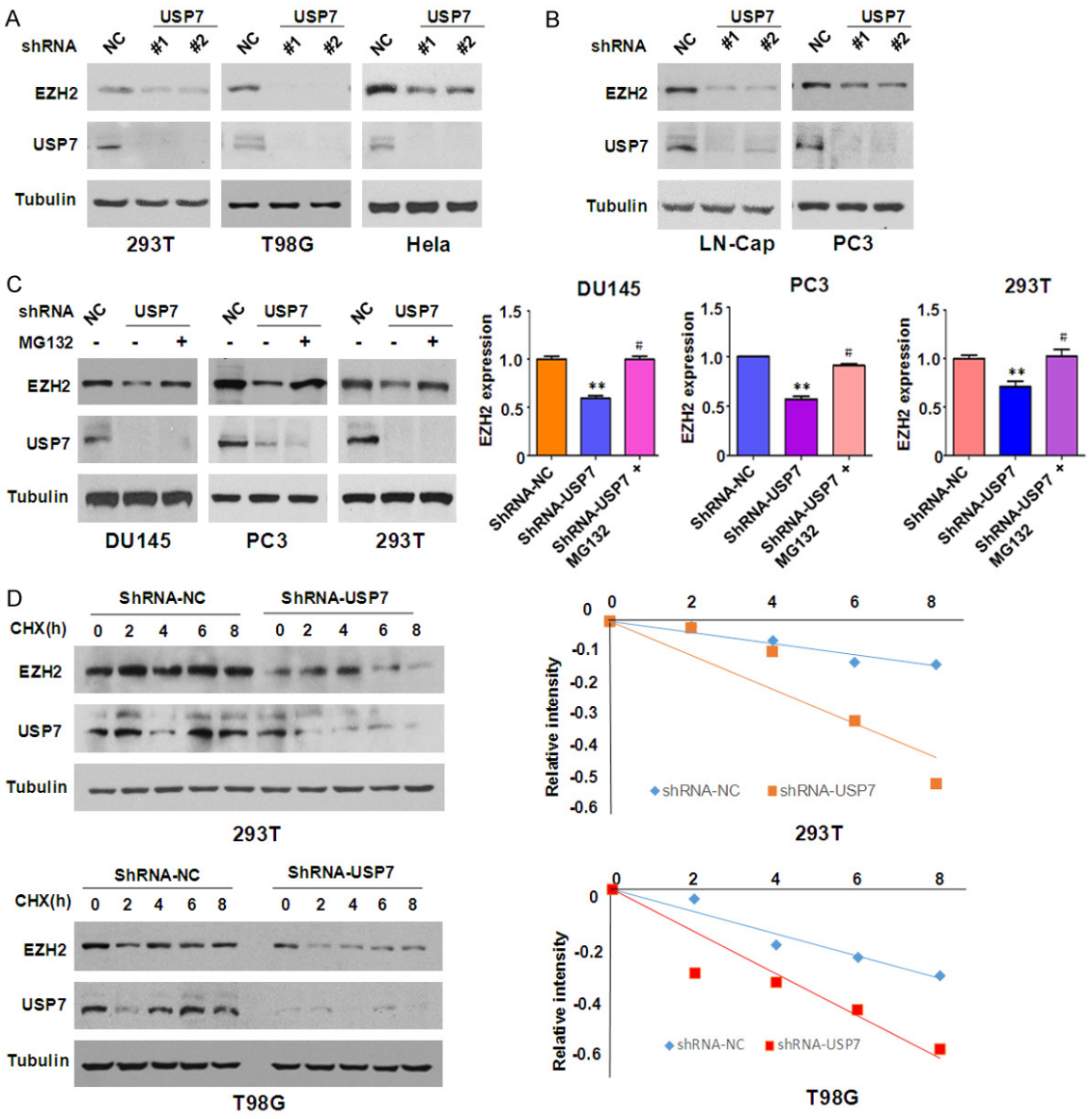

Figure 2. USP7 promotes the stabilization of EZH2. (A) 293T, T98G and HeLa cells were transfected with control shRNA or different sets of USP7 shRNAs. Cellular extracts were analyzed by Western blotting. (B) Experiments analogous to those in part (A) were performed in prostate cancer LNCaP and PC3 cell lines. (C) Left panel, DU145, PC3 and 293T cells were transfected with control shRNA or USP7 shRNA and then treated with DMSO or the proteasome inhibitor MG132 (10 μM). The cells were harvested and analyzed by Western blotting. Right panel, Quantitative results are illustrated for the left panel. (D) Left panel, 293T or T98G cells were transfected with control shRNA or USP7 shRNA, followed by addition of cycloheximide (CHX 50 μg/ml), and collected at different time points. Then, the samples were detected by IB. Right panel, Quantitative results are illustrated for the left panel.

time points and Western blotting result showed that the half-life of EZH2 was markedly reduced due to the knockdown of USP7 (**Figure 2D**). Taken together, these data demonstrated that USP7 regulated the stability of EZH2.

USP7 deubiquitinates EZH2

Next, we detected whether the EZH2 stability promoted by USP7 was a result of EZH2 deubiquitination mediated by USP7. 293T and HeLa cells were cotransfected with Myc-EZH2, HA-ub and Flag-USP7. The results of IP with Myc beads followed by IB with anti-HA antibody showed that overexpression of USP7 mediated the decreased ubiquitination of EZH2 in 293T cells (**Figure 3A**). The similar results were observed in HeLa cells (**Figure 3B**). Moreover, 293T cells were transfected with Myc-EZH2, HA-ub and USP7-shRNA. IP of the celluar

lysates with Myc beads followed by IB with HA antibody suggested that deletion of USP7 increased the ubiquitination of EZH2 (**Figure 3C**). Similar results were observed in HeLa cells. IB with the antiub antibody indicated that USP7 knockdown promoted EZH2 ubiquitination (**Figure 3D**). To further ascertain whether the EZH2 stabilization promoted by USP7 is dependent on the enzymatic activity of USP7, we transfected the HeLa and 293T cells with mutant USP7/C223S or wild-type USP7. Western blotting analysis showed that EZH2 ubiquitination was increased in cells that had been transfected with USP7/C223S compared with that in cells transfected with wild-type USP7 (**Figure 3E**, **3F**). Altogether, these results suggest that the stabilization of EZH2 promoted by USP7 is a consequence of USP7-mediated EZH2 deubiquitination.

USP7 promotes cell growth, cell migration and invasion

To investigate the function of the interaction between USP7 and EZH2, we performed a series of experiments in PC3 and DU145 prostate cancer cells. The prostate cancer cells were seeded into a 96-well plate and transfected with USP7 cDNA or USP7-shRNA and control vector. Then, 20 μl of CTG was added to each well and the results revealed that USP7 overexpression promoted cell proliferation, while the knock down of USP7 inhibited cell growth in prostate cancer cells (**Figure 4A**). The data indicated that USP7 overexpression promoted cell proliferation in prostate cancer cells. To further address the role of the USP7-EZH2 axis in prostate cancer cells, a migration assay was performed in PC3 and DU145 cells after transfection of USP7 cDNA, USP7-shRNA or control vector. Cellular migration was promoted by USP7 overexpression, and the number of cells that migrated into the scratch increased in both prostate cancer cell lines (**Figure 4B**). Moreover, the number of cells that migrated significantly decreased with USP7 knockdown in DU145 and PC3 cells (**Figure 4C**). Our data indicate that the migratory activity of prostate cancer cells was regulated by USP7. Next, we applied an invasion assay to detect the effect of USP7 overexpression on invasive ability. Our results showed that the number of cells that had invaded through the Matrigel-coated membrane was increased with USP7 overexpression (**Figure 4D**). When USP7 was deficient, cell invasion was decreased in PC3 and DU145 cells (**Figure 4E**). These results indicate that USP7 overexpression significantly promotes invasive activity in prostate cancer cells.

The USP7-EZH2 axis promotes cell migration, invasion and apoptosis

To further confirm the function of the USP7-EZH2 axis in prostate cancer cells, we transfected USP7 cDNA, EZH2-shRNA or a combination of both plasmids into prostate cancer cells, respectively. We found that the USP7 overexpression increased the number of migratory cells, while knockdown of EZH2 abolished migratory activity caused by USP7 overexpression (**Figure 5A**, **5B**). Invasion assay was conducted to investigate the role of the interaction of USP7 and EZH2 in prostate cancer cell invasion. The data showed that the number of invasive cells was increased as a result of the USP7 overexpression, suggesting that USP7 overexpression improved the activity of cell invasion. The EZH2 knockdown antagonized the increased activity of cells caused by USP7 upregulation (**Figure 5C**, **5D**). Next, we further dissected whether USP7-mediated cell apoptosis could be reversed by the downregulation of EZH2. In PC3 cells, the proportion of apoptotic cells decreased from 10% to 5.82% with USP7 overexpression, while the EZH2 deficiency converted the proportion of apoptotic cells to 10.54% (**Figure 5E**). These results indicate that USP7 inhibits cell apoptosis via EZH2 stabilization in prostate cancer cells.

USP7 downregulation suppresses prostate carcinogenesis in vivo

We constructed a stable USP7 knockdown cell line using USP7-shRNA in PC3 cells and injected the cells into nude mice with the same number of control cells. During the following weeks, the weight of mice and the volume of tumors were measured once every 2 d. Then, the mice were killed, and the tumors were resected, and the weight and size of the tumors were recorded (**Figure 6A**). According to the results, the volume of the tumors in the USP7 deletion group was much lower than that in the control group (**Figure 6**). Moreover, the weights of mice in the two groups were not sub-

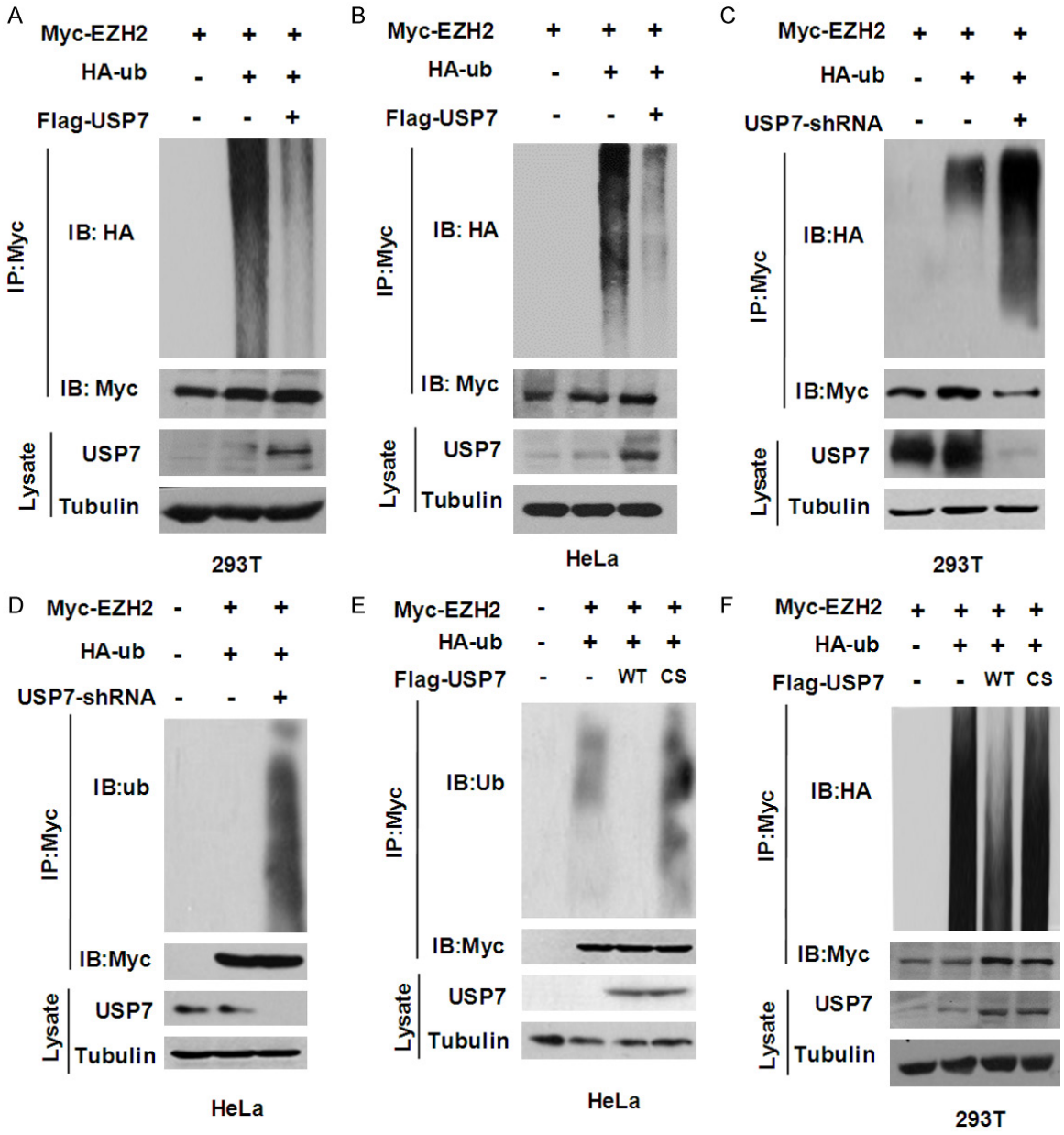

Figure 3. USP7 deubiquitinates EZH2. (A) 293T cells were transfected with Flag-USP7, HA-Ub or Myc-EZH2 as indicated. The harvested cells were immunoprecipitated with anti-Myc followed by IB with anti-HA or anti-Ub. (B) Experiments analogous to those in part (A) were performed in HeLa cells. (C) 293T cells were transfected with HA-ub, Myc-EZH2, control shRNA or USP7 shRNA. Then, the cells were collected cells and the extracts were immunoprecipitated with anti-Myc followed by IB with anti-HA. (D) Experiments analogous to those in part (C) were performed in HeLa cells with anti-Ub. (E, F) HeLa cells (E) and 293T cells (F) were transfected with Myc-EZH2 or HA-Ub and Flag-USP7/WT or Flag-USP7/C223S. The harvested cells were immunoprecipitated with anti-Myc followed by IB with anti-HA.

stantially different (**Figure 6B**). To investigate the role of USP7 overexpression in carcinogenesis in depth, we performed mouse experiments. To this end, we established stable USP7-overexpressing cell lines using PC3 cells. USP7-overexpressing cells and control cells were injected into nude mice. Tumor growth and mouse weight were monitored for approximately about 6 weeks. Then the mice were killed and tumors were resected. Notably, the tumor growth and volume were greatly increased in USP7-overexpressing group (**Figure 6C**). Moverover, the weight of mice did not differ between these two groups (**Figure**

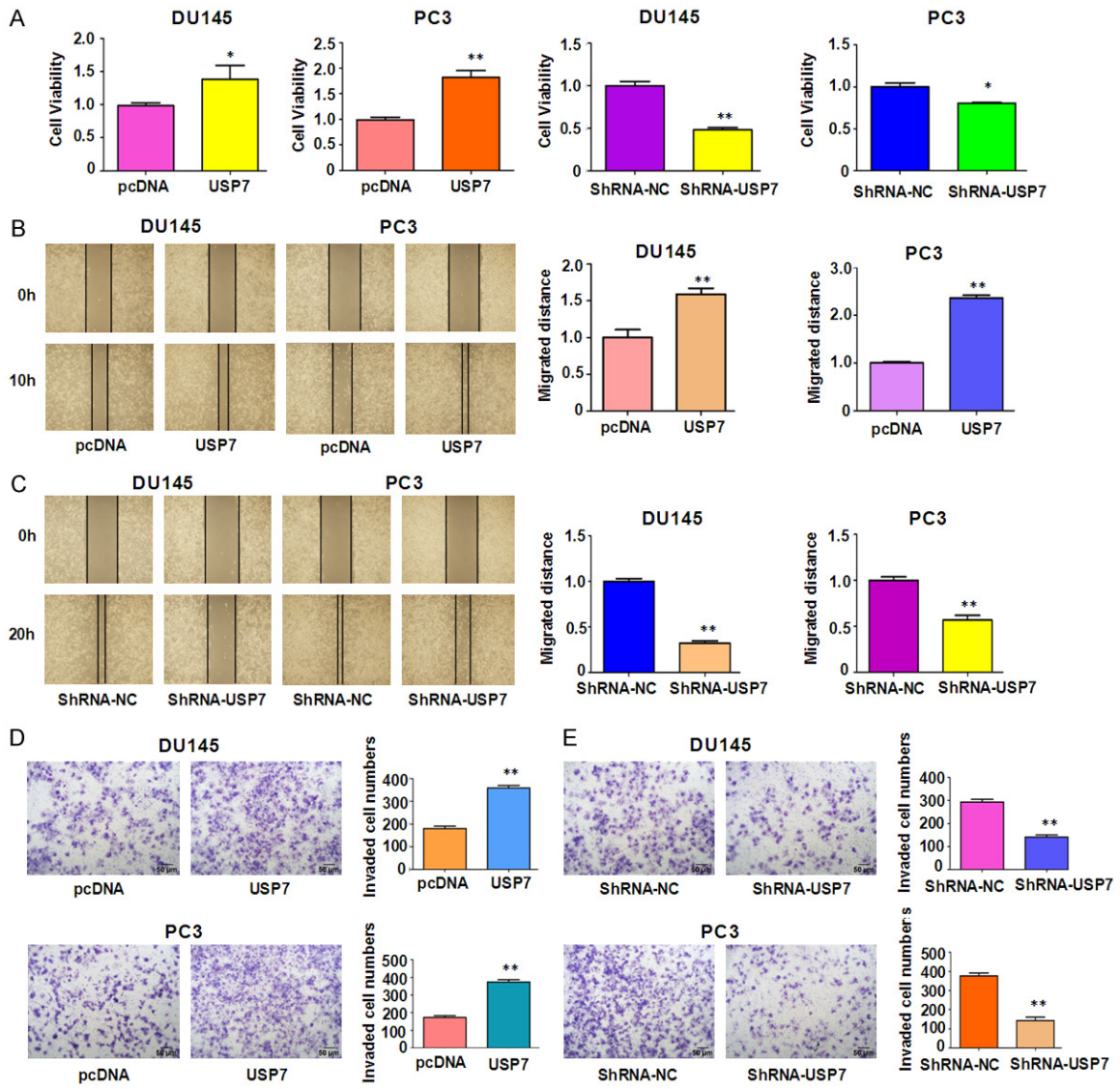

Figure 4. USP7 promotes cell growth, cell migration and invasion. A. Prostate cancer cells were transfected with USP7 cDNA, shRNA-USP7, empty vector or control shRNA. A CTG assay was performed to measure cell proliferation in prostate cancer cells. *P<0.05, **P<0.01. B, C. Left panel, A wound healing assay was performed in DU145 and PC3 cells that had been trnasfected with USP7 cDNA or shRNA-USP7. Right panel, Quantitative results are illustrated for the left panel. **P<0.01 vs empty vector or control shRNA. D, E. Left panel, DU145 and PC3 cells were transfected with USP7 cDNA, shRNA-USP7, empty vector or control shRNA. Cell invasion was detected by Transwell chambers assay in prostate cancer cells. Right panel: quantitative results are illustrated for the left panel. **P<0.01 vs empty vector or control shRNA.

6D). The immunohistochemical staining was performed on the resected tumors. We found that the staining of USP7 and EZH2 was much heavier in the USP7 overexpressing group than that in the control group, which suggested that USP7 and EZH2 were highly expressed in USP7-overexpressing tissues (**Figure 6E**). Collectively, these results strongly support a role of the USP7-EZH2 axis in promoting prostate carcinogenesis.

A correlation between USP7 and EZH2 expression is observed in prostate cancer tumor tissues

To further investigate the clinical relevance of USP7 and EZH2 in prostate cancer, we stained prostate cancer tissues for USP7 and EZH2. We found that USP7 was overexpressed in most prostate cancer clinical tissues. Moreover, we identified a correlation between USP7 and

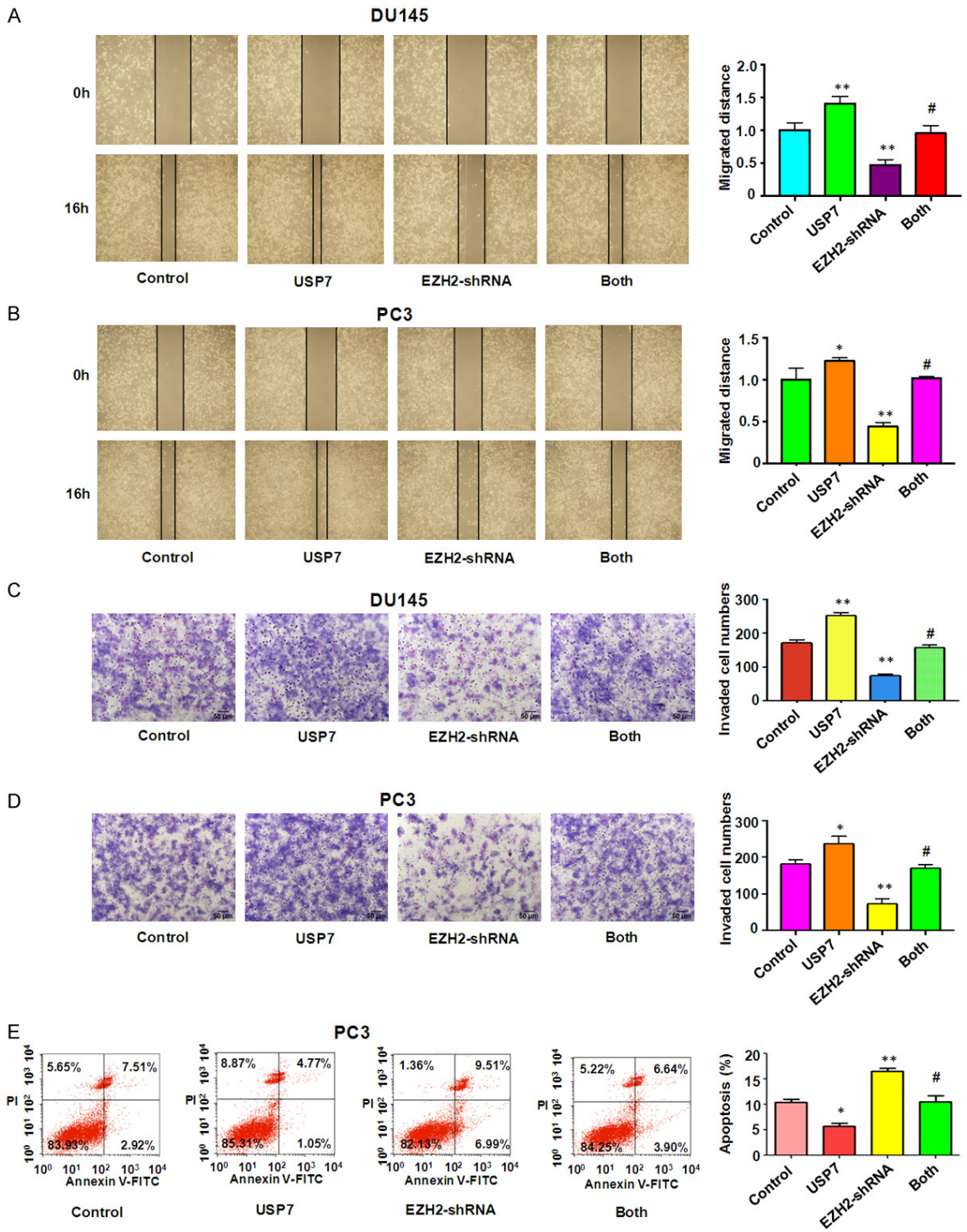

Figure 5. The USP7-EZH2 axis promotes cell migration, invasion and apoptosis. A, B. Left panel, DU145 (A) and PC3 (B) cells were transfected with empty vector, USP7, EZH2-shRNA, or a combination of USP7 and EZH2-shRNA. Then, the cells were analyzed by the wound healing assay. Right panel, Quantitative results are illustrated for the left panel. **P*<0.05 vs control, ***P*<0.01 vs control. #*P*<0.05 vs USP7 or EZH2-shRNA. C, D. Left panel, Transwell chamber assays were performed with DU145 (C) and PC3 (D) cells that had been transfected with empty vector or USP7, EZH2-shRNA, or a combination of USP7 transfection and EZH2-shRNA. Right panel, Quantitative results are illustrated for the left panel. E. Cell apoptosis was analyzed by FACS in PC3 and DU145 cells after transfection with empty vector, USP7, EZH2-shRNA, or a combination of USP7 transfection and EZH2-shRNA.

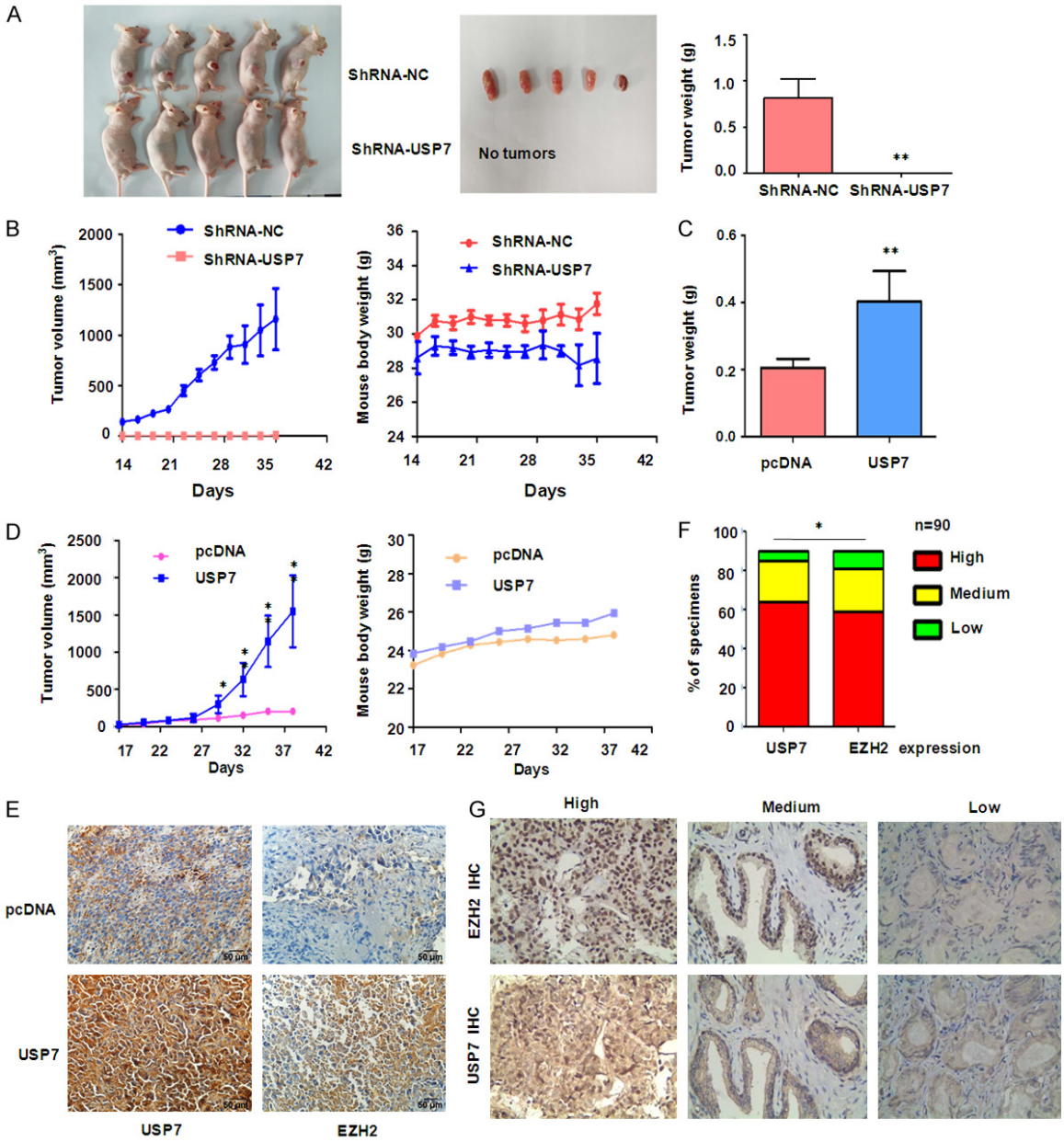

Figure 6. USP7 deletion suppresses prostate carcinogenesis in vivo. A: PC3 cancer cells stably expressing USP7 shRNA and control shRNA as indicated were transplanted into nude mice. Representative mice were shown. $^{**}P<0.01$. B: The resected tumors were shown and the tumor weight was measured. $^{**}P<0.01$. The tumor volumes and mouse weight were measured every 2 d. C: PC3 cells stably overexpressing USP7 were transplanted onto nude mice. The PC3 tumors stably overexpressing USP7 were measured every 4 d, and the tumor weights were shown. D: Left panel: the tumor volumes were measured. $^{*}P<0.05$. Right: panel: the weight of mice in both groups was detected. E: The resected tumors were analyzed by IHC. F: Statistical analyses of the correlation between USP7 and EZH2 expression in prostate cancer tissue microarrays were performed. G: Representative images of USP7 and EZH2 IHC from 90 cases of prostate cancer were shown.

EZH2 expression in prostate cancer tumor tissue (**Figure 6F**, **6G**).

Discussion

Emerging evidence has demonstrated that USP7 plays a crucial role in tumorigenesis [13, 26]. USP7 has been identified as a specific deubiquitinase for both p53 and Mdm2, and regulates p53 stabilization [27-29]. In line with this, one study showed that reduction in USP7 expression enhanced NSCLC (non-small cell lung cancer) carcinogenesis via a p53-depen-

dent pathway [30]. Moreover, USP7 regulates the ubiquitination state of RING1B, resulting in its stabilization [31]. Furthermore, Song et al found that the deubiquitinylation and localization of PTEN are regulated by a USP7-PML network [32]. Additionally, USP7 accelerates p14 degradation by deubiquitinating TRIP12 (thyroid hormone receptor-interacting protein 12) and promotes hepatocellular carcinoma progression [33]. Notably, stabilization of the histone demethylase PHF8 by USP7 promotes breast carcinogenesis [34]. Strikingly, USP7 was found to deubiquitinate and stabilize N-Myc in neuroblastoma [35]. Here, we found that USP2 deubiquitinated and stabilized EZH2 in prostate cancer cells.

EZH2 has been reported to have function in the progression of PCa [16], yet the exact mechanism remains elusive. In this study, from mouse xenograft and human PCa cells, we uncovered that USP7 plays a functional role in the elevation of EZH2 in PCa. The histone methylase EZH2 interacts with the deubiquitinase USP7 and is stabilized by it. Importantly, our results support a model in which USP7 overexpression results in a high level of EZH2 in PCa, and USP7 and EZH2 synergistically drive the tumorigenesis of PCa via deregulation of targeted genes. USP7 overexpression is associated with poor outcome in patients with glioma [36]. Similarly, USP7 overexpression correlated with malignant phenotype in lung squamous cell carcinoma and large cell carcinoma, suggesting that high USP7 levels predict a poor prognosis in lung cancer [37]. It has been found that overexpression of USP7 is correlated with poor prognosis in epithelial ovarian cancer [38, 39]. Notably, USP7 is overexpressed in prostate cancer and high levels of USP7 are directly associated with tumor aggressiveness [32]. Exploration whether the expression of USP7 in prostate tumor samples is associated with EZH2 levels is needed.

Several USP7 inhibitors have been developed for cancer treatment [40, 41]. For example, two vIRF4 (viral interferon regulatory factor 4)-derived peptides, vif1 and vif2, have been characrized as potent and selective USP7 antagonists [42]. Specifically, the vif1 peptide binds the USP7 TRAF domain to block substrate binding, whereas the vif2 peptide binds the TRAF and catalytic domains of USP7 to inhibit its deubiquitination activity [42]. These two peptide treatments led to p53-dependent cell cycle arrest and apoptosis and tumor regression due to blockade of USP7 [42]. Moreover, HBX 41,108, a small-molecular compound that inhibits deubiquitinating activity of USP7, induced elevated p53 and apoptosis in cancer cell lines [43, 44]. Later, HBX 19,818 and HBX 28,258 were identified as USP7 inhibitors [45]. The USP7 inhibitor P22077 inhibits neuroblastoma growth by inducing p53-induced apoptosis [46]. Interestingly, spongiacidin C, a pyrrole alkaloid from the marine sponge stylissa massa, has been validated to be a USP7 inhibitor [47]. P5091, an inhibitor of USP7, induced apoptosis in multiple myeloma cells, inhibited tumor growth and prolonged survival [48]. Combining P5091 with lenalidomide or dexamethasone led to synergistic anti-multiple myeloma activity [48]. In line with this phenomenon, P5091 sensitizes cells to PARP-inhibitor drugs in lung neuroendocrine cancer cells [49]. One study also showed that P5091 inhibits Wnt signaling and colorectal tumor growth [50]. P22077 and P5091 induce apoptosis through oxidative and endoplasmic reticulum stress in human cancer cells [51]. Recently, P5091 was shown to sensitize cells to PARP inhibitors in hormone-sensitive and castration-resistant prostate cancer [52], suggesting that USP7 inhibitors could be useful for the treatment of human advanced prostate cancer.

Taken together, our work demonstrated a novel mechanism which EZH2 serves as a substrate for USP7 and showed that the stability of EZH2 is regulated by the deubiquitinase USP7 via deubiquitination in prostate tumorigenesis. Our results revealed that overexpression of USP7 could increase the metastatic invasive activity and enhance carcinogenesis in mice via stabilization of EZH2, which indicated that the USP7/EZH2 axis is critically involved in prostate cancer tumorigenesis. Therefore, targeting USP7/EZH2 could be a new therapeutic strategy to control the growth of prostate cancer.

Acknowledgements

This work was supported by Research Fund for Lin He's Academician Workstation of New Medicine and Clinical Translation and Science and Technology Planning Project of Wenzhou city (No. Y20180082).

Disclosure of conflict of interest

None.

Address correspondence to: Zhiwei Wang, Department of Obstetrics and Gynecology, The Second Affiliated Hospital of Wenzhou Medical University, Wenzhou 325027, Zhejiang Province, China. E-mail: zwang6@bidmc.harvard.edu; Youhua He, Department of Urology, The Second Affiliated Hospital, Wenzhou Medical University, Wenzhou 325027, Zhejiang Province, China. E-mail: feymnwk@126.com

References

[1] Siegel RL, Miller KD and Jemal A. Cancer statistics, 2018. CA Cancer J Clin 2018; 68: 7-30.

[2] Carroll PR, Parsons JK, Andriole G, Bahnson RR, Castle EP, Catalona WJ, Dahl DM, Davis JW, Epstein JI, Etzioni RB, Farrington T, Hemstreet GP 3rd, Kawachi MH, Kim S, Lange PH, Loughlin KR, Lowrance W, Maroni P, Mohler J, Morgan TM, Moses KA, Nadler RB, Poch M, Scales C, Shaneyfelt TM, Smaldone MC, Sonn G, Sprenkle P, Vickers AJ, Wake R, Shead DA and Freedman-Cass DA. NCCN guidelines insights: prostate cancer early detection, version 2.2016. J Natl Compr Canc Netw 2016; 14: 509-519.

[3] Schröder FH, Hugosson J, Roobol MJ, Tammela TL, Ciatto S, Nelen V, Kwiatkowski M, Lujan M, Lilja H, Zappa M, Denis LJ, Recker F, Páez A, Määttänen L, Bangma CH, Aus G, Carlsson S, Villers A, Rebillard X, van der Kwast T, Kujala PM, Blijenberg BG, Stenman UH, Huber A, Taari K, Hakama M, Moss SM, de Koning HJ and Auvinen A; ERSPC Investigators. Prostate-cancer mortality at 11 years of follow-up. N Engl J Med 2012; 366: 981-990.

[4] Nalepa G, Rolfe M and Harper JW. Drug discovery in the ubiquitin-proteasome system. Nat Rev Drug Discov 2006; 5: 596-613.

[5] Zheng N, Zhou Q, Wang Z and Wei W. Recent advances in SCF ubiquitin ligase complex: clinical implications. Biochim Biophys Acta 2016; 1866: 12-22.

[6] Zhou J, Wang J, Chen C, Yuan H, Wen X and Sun H. USP7: target validation and drug discovery for cancer therapy. Med Chem 2018; 14: 3-18.

[7] Bedford L, Lowe J, Dick LR, Mayer RJ and Brownell JE. Ubiquitin-like protein conjugation and the ubiquitin-proteasome system as drug targets. Nat Rev Drug Discov 2011; 10: 29-46.

[8] Reyes-Turcu FE, Ventii KH and Wilkinson KD. Regulation and cellular roles of ubiquitin-specific deubiquitinating enzymes. Annu Rev Biochem 2009; 78: 363-397.

[9] Komander D, Clague MJ and Urbe S. Breaking the chains: structure and function of the deubiquitinases. Nat Rev Mol Cell Biol 2009; 10: 550-563.

[10] Liang J, Saad Y, Lei T, Wang J, Qi D, Yang Q, Kolattukudy PE and Fu M. MCP-induced protein 1 deubiquitinates TRAF proteins and negatively regulates JNK and NF-kappaB signaling. J Exp Med 2010; 207: 2959-2973.

[11] Fraile JM, Quesada V, Rodríguez D, Freije JM and López-Otín C. Deubiquitinases in cancer: new functions and therapeutic options. Oncogene 2012; 31: 2373-2388.

[12] Everett RD, Meredith M, Orr A, Cross A, Kathoria M and Parkinson J. A novel ubiquitin-specific protease is dynamically associated with the PML nuclear domain and binds to a herpesvirus regulatory protein. EMBO J 1997; 16: 566-577.

[13] Li M, Chen D, Shiloh A, Luo J, Nikolaev AY, Qin J and Gu W. Deubiquitination of p53 by HAUSP is an important pathway for p53 stabilization. Nature 2002; 416: 648-653.

[14] Kategaya L, Di Lello P, Rougé L, Pastor R, Clark KR, Drummond J, Kleinheinz T, Lin E, Upton JP, Prakash S, Heideker J, McCleland M, Ritorto MS, Alessi DR, Trost M, Bainbridge TW, Kwok MCM, Ma TP, Stiffler Z, Brasher B, Tang Y, Jaishankar P, Hearn BR, Renslo AR, Arkin MR, Cohen F, Yu K, Peale F, Gnad F, Chang MT, Klijn C, Blackwood E, Martin SE, Forrest WF, Ernst JA, Ndubaku C, Wang X, Beresini MH, Tsui V, Schwerdtfeger C, Blake RA, Murray J, Maurer T and Wertz IE. USP7 small-molecule inhibitors interfere with ubiquitin binding. Nature 2017; 550: 534-538.

[15] Chung WH, Hung SI, Hong HS, Hsih MS, Yang LC, Ho HC, Wu JY and Chen YT. Medical genetics: a marker for Stevens-Johnson syndrome. Nature 2004; 428: 486.

[16] Varambally S, Dhanasekaran SM, Zhou M, Barrette TR, Kumar-Sinha C, Sanda MG, Ghosh D, Pienta KJ, Sewalt RG, Otte AP, Rubin MA and Chinnaiyan AM. The polycomb group protein EZH2 is involved in progression of prostate cancer. Nature 2002; 419: 624-629.

[17] Xu K, Wu ZJ, Groner AC, He HH, Cai C, Lis RT, Wu X, Stack EC, Loda M, Liu T, Xu H, Cato L, Thornton JE, Gregory RI, Morrissey C, Vessella RL, Montironi R, Magi-Galluzzi C, Kantoff PW, Balk SP, Liu XS and Brown M. EZH2 oncogenic activity in castration-resistant prostate cancer cells is polycomb-independent. Science 2012; 338: 1465-1469.

[18] Yu J, Cao Q, Mehra R, Laxman B, Yu J, Tomlins SA, Creighton CJ, Dhanasekaran SM, Shen R, Chen G, Morris DS, Marquez VE, Shah RB, Ghosh D, Varambally S and Chinnaiyan AM. Integrative genomics analysis reveals silencing

of beta-adrenergic signaling by polycomb in prostate cancer. Cancer Cell 2007; 12: 419-431.
[19] Chen H, Tu SW and Hsieh JT. Down-regulation of human DAB2IP gene expression mediated by polycomb Ezh2 complex and histone deacetylase in prostate cancer. J Biol Chem 2005; 280: 22437-22444.
[20] Min J, Zaslavsky A, Fedele G, McLaughlin SK, Reczek EE, De Raedt T, Guney I, Strochlic DE, Macconaill LE, Beroukhim R, Bronson RT, Ryeom S, Hahn WC, Loda M and Cichowski K. An oncogene-tumor suppressor cascade drives metastatic prostate cancer by coordinately activating Ras and nuclear factor-kappaB. Nat Med 2010; 16: 286-294.
[21] Lu W, Liu S, Li B, Xie Y, Izban MG, Ballard BR, Sathyanarayana SA, Adunyah SE, Matusik RJ and Chen Z. SKP2 loss destabilizes EZH2 by promoting TRAF6-mediated ubiquitination to suppress prostate cancer. Oncogene 2017; 36: 1364-1373.
[22] Sahasrabuddhe AA, Chen X, Chung F, Velusamy T, Lim MS and Elenitoba-Johnson KS. Oncogenic Y641 mutations in EZH2 prevent Jak2/beta-TrCP-mediated degradation. Oncogene 2015; 34: 445-454.
[23] Zoabi M, Sadeh R, de Bie P, Marquez VE and Ciechanover A. PRAJA1 is a ubiquitin ligase for the polycomb repressive complex 2 proteins. Biochem Biophys Res Commun 2011; 408: 393-398.
[24] Shen Z, Chen L, Yang X, Zhao Y, Pier E, Zhang X, Yang X and Xiong Y. Downregulation of Ezh2 methyltransferase by FOXP3: new insight of FOXP3 into chromatin remodeling? Biochim Biophys Acta 2013; 1833: 2190-2200.
[25] Yu YL, Chou RH, Shyu WC, Hsieh SC, Wu CS, Chiang SY, Chang WJ, Chen JN, Tseng YJ, Lin YH, Lee W, Yeh SP, Hsu JL, Yang CC, Hung SC and Hung MC. Smurf2-mediated degradation of EZH2 enhances neuron differentiation and improves functional recovery after ischaemic stroke. EMBO Mol Med 2013; 5: 531-547.
[26] Bhattacharya S, Chakraborty D, Basu M and Ghosh MK. Emerging insights into HAUSP (USP7) in physiology, cancer and other diseases. Signal Transduct Target Ther 2018; 3: 17.
[27] Brooks CL, Li M, Hu M, Shi Y and Gu W. The p53--Mdm2--HAUSP complex is involved in p53 stabilization by HAUSP. Oncogene 2007; 26: 7262-7266.
[28] Sheng Y, Saridakis V, Sarkari F, Duan S, Wu T, Arrowsmith CH and Frappier L. Molecular recognition of p53 and MDM2 by USP7/HAUSP. Nat Struct Mol Biol 2006; 13: 285-291.
[29] Li M, Brooks CL, Kon N and Gu W. A dynamic role of HAUSP in the p53-Mdm2 pathway. Mol Cell 2004; 13: 879-886.
[30] Masuya D, Huang C, Liu D, Nakashima T, Yokomise H, Ueno M, Nakashima N and Sumitomo S. The HAUSP gene plays an important role in non-small cell lung carcinogenesis through p53-dependent pathways. J Pathol 2006; 208: 724-732.
[31] de Bie P, Zaaroor-Regev D and Ciechanover A. Regulation of the polycomb protein RING1B ubiquitination by USP7. Biochem Biophys Res Commun 2010; 400: 389-395.
[32] Song MS, Salmena L, Carracedo A, Egia A, Lo-Coco F, Teruya-Feldstein J and Pandolfi PP. The deubiquitinylation and localization of PTEN are regulated by a HAUSP-PML network. Nature 2008; 455: 813-817.
[33] Cai JB, Shi GM, Dong ZR, Ke AW, Ma HH, Gao Q, Shen ZZ, Huang XY, Chen H, Yu DD, Liu LX, Zhang PF, Zhang C, Hu MY, Yang LX, Shi YH, Wang XY, Ding ZB, Qiu SJ, Sun HC, Zhou J, Shi YG and Fan J. Ubiquitin-specific protease 7 accelerates p14(ARF) degradation by deubiquitinating thyroid hormone receptor-interacting protein 12 and promotes hepatocellular carcinoma progression. Hepatology 2015; 61: 1603-1614.
[34] Wang Q, Ma S, Song N, Li X, Liu L, Yang S, Ding X, Shan L, Zhou X, Su D, Wang Y, Zhang Q, Liu X, Yu N, Zhang K, Shang Y, Yao Z and Shi L. Stabilization of histone demethylase PHF8 by USP7 promotes breast carcinogenesis. J Clin Invest 2016; 126: 2205-2220.
[35] Tavana O, Li D, Dai C, Lopez G, Banerjee D, Kon N, Chen C, Califano A, Yamashiro DJ, Sun H and Gu W. HAUSP deubiquitinates and stabilizes N-Myc in neuroblastoma. Nat Med 2016; 22: 1180-1186.
[36] Cheng C, Niu C, Yang Y, Wang Y and Lu M. Expression of HAUSP in gliomas correlates with disease progression and survival of patients. Oncol Rep 2013; 29: 1730-1736.
[37] Zhao GY, Lin ZW, Lu CL, Gu J, Yuan YF, Xu FK, Liu RH, Ge D and Ding JY. USP7 overexpression predicts a poor prognosis in lung squamous cell carcinoma and large cell carcinoma. Tumour Biol 2015; 36: 1721-1729.
[38] Zhang L, Wang H, Tian L and Li H. Expression of USP7 and MARCH7 is correlated with poor prognosis in epithelial ovarian cancer. Tohoku J Exp Med 2016; 239: 165-175.
[39] Ma M and Yu N. Ubiquitin-specific protease 7 expression is a prognostic factor in epithelial ovarian cancer and correlates with lymph node metastasis. Onco Targets Ther 2016; 9: 1559-1569.
[40] Turnbull AP, Ioannidis S, Krajewski WW, Pinto-Fernandez A, Heride C, Martin ACL, Tonkin LM, Townsend EC, Buker SM, Lancia DR, Caravella JA, Toms AV, Charlton TM, Lahdenranta J, Wilker E, Follows BC, Evans NJ, Stead L, Alli C,

Zarayskiy VV, Talbot AC, Buckmelter AJ, Wang M, McKinnon CL, Saab F, McGouran JF, Century H, Gersch M, Pittman MS, Marshall CG, Raynham TM, Simcox M, Stewart LMD, McLoughlin SB, Escobedo JA, Bair KW, Dinsmore CJ, Hammonds TR, Kim S, Urbé S, Clague MJ, Kessler BM and Komander D. Molecular basis of USP7 inhibition by selective small-molecule inhibitors. Nature 2017; 550: 481-486.

[41] Gavory G, O'Dowd CR, Helm MD, Flasz J, Arkoudis E, Dossang A, Hughes C, Cassidy E, McClelland K, Odrzywol E, Page N, Barker O, Miel H and Harrison T. Discovery and characterization of highly potent and selective allosteric USP7 inhibitors. Nat Chem Biol 2018; 14: 118-125.

[42] Lee HR, Choi WC, Lee S, Hwang J, Hwang E, Guchhait K, Haas J, Toth Z, Jeon YH, Oh TK, Kim MH and Jung JU. Bilateral inhibition of HAUSP deubiquitinase by a viral interferon regulatory factor protein. Nat Struct Mol Biol 2011; 18: 1336-1344.

[43] Weinstock J, Wu J, Cao P, Kingsbury WD, McDermott JL, Kodrasov MP, McKelvey DM, Suresh Kumar KG, Goldenberg SJ, Mattern MR and Nicholson B. Selective dual inhibitors of the cancer-related deubiquitylating proteases USP7 and USP47. ACS Med Chem Lett 2012; 3: 789-792.

[44] Colland F, Formstecher E, Jacq X, Reverdy C, Planquette C, Conrath S, Trouplin V, Bianchi J, Aushev VN, Camonis J, Calabrese A, Borg-Capra C, Sippl W, Collura V, Boissy G, Rain JC, Guedat P, Delansorne R and Daviet L. Small-molecule inhibitor of USP7/HAUSP ubiquitin protease stabilizes and activates p53 in cells. Mol Cancer Ther 2009; 8: 2286-2295.

[45] Reverdy C, Conrath S, Lopez R, Planquette C, Atmanene C, Collura V, Harpon J, Battaglia V, Vivat V, Sippl W and Colland F. Discovery of specific inhibitors of human USP7/HAUSP deubiquitinating enzyme. Chem Biol 2012; 19: 467-477.

[46] Fan YH, Cheng J, Vasudevan SA, Dou J, Zhang H, Patel RH, Ma IT, Rojas Y, Zhao Y, Yu Y, Zhang H, Shohet JM, Nuchtern JG, Kim ES and Yang J. USP7 inhibitor P22077 inhibits neuroblastoma growth via inducing p53-mediated apoptosis. Cell Death Dis 2013; 4: e867.

[47] Yamaguchi M, Miyazaki M, Kodrasov MP, Rotinsulu H, Losung F, Mangindaan RE, de Voogd NJ, Yokosawa H, Nicholson B and Tsukamoto S. Spongiacidin C, a pyrrole alkaloid from the marine sponge Stylissa massa, functions as a USP7 inhibitor. Bioorg Med Chem Lett 2013; 23: 3884-3886.

[48] Chauhan D, Tian Z, Nicholson B, Kumar KG, Zhou B, Carrasco R, McDermott JL, Leach CA, Fulcinniti M, Kodrasov MP, Weinstock J, Kingsbury WD, Hideshima T, Shah PK, Minvielle S, Altun M, Kessler BM, Orlowski R, Richardson P, Munshi N and Anderson KC. A small molecule inhibitor of ubiquitin-specific protease-7 induces apoptosis in multiple myeloma cells and overcomes bortezomib resistance. Cancer Cell 2012; 22: 345-358.

[49] Malapelle U, Morra F, Ilardi G, Visconti R, Merolla F, Cerrato A, Napolitano V, Monaco R, Guggino G, Monaco G, Staibano S, Troncone G and Celetti A. USP7 inhibitors, downregulating CCDC6, sensitize lung neuroendocrine cancer cells to PARP-inhibitor drugs. Lung Cancer 2017; 107: 41-49.

[50] An T, Gong Y, Li X, Kong L, Ma P, Gong L, Zhu H, Yu C, Liu J, Zhou H, Mao B and Li Y. USP7 inhibitor P5091 inhibits Wnt signaling and colorectal tumor growth. Biochem Pharmacol 2017; 131: 29-39.

[51] Lee G, Oh TI, Um KB, Yoon H, Son J, Kim BM, Kim HI, Kim H, Kim YJ, Lee CS and Lim JH. Small-molecule inhibitors of USP7 induce apoptosis through oxidative and endoplasmic reticulum stress in cancer cells. Biochem Biophys Res Commun 2016; 470: 181-186.

[52] Morra F, Merolla F, Napolitano V, Ilardi G, Miro C, Paladino S, Staibano S, Cerrato A and Celetti A. The combined effect of USP7 inhibitors and PARP inhibitors in hormone-sensitive and castration-resistant prostate cancer cells. Oncotarget 2017; 8: 31815-31829.

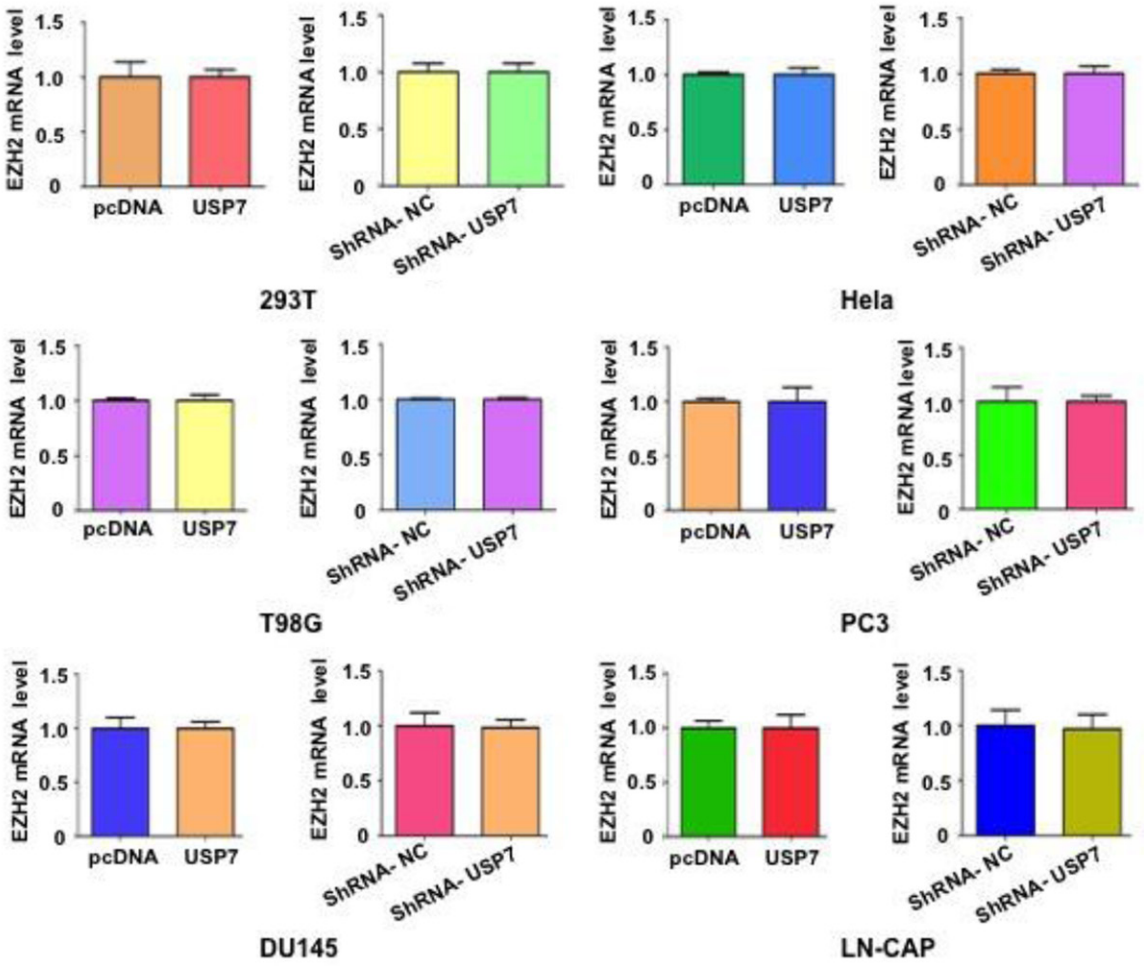

Supplementary Figure 1. QT-PCR was performed in PC3, DU145, LNCaP, 293T, HeLa and T98G cells with empty vector or USP7 cDNA or control shRNA or USP7 shRNA transfection.